

This article was downloaded by:[Bochkarev, N.]
On: 19 December 2007
Access Details: [subscription number 788631019]
Publisher: Taylor & Francis
Informa Ltd Registered in England and Wales Registered Number: 1072954
Registered office: Mortimer House, 37-41 Mortimer Street, London W1T 3JH, UK



Astronomical & Astrophysical Transactions

The Journal of the Eurasian Astronomical Society

Publication details, including instructions for authors and subscription information:
<http://www.informaworld.com/smpp/title~content=t713453505>

The outflow regime of quasispherical accretion onto a compact X-ray object

Igor V. Igumenshchev ^a; Andrei F. Illarionov ^b; Dmitrii A. Kompaneets ^b

^a Institute of Astronomy, Moscow, Russia

^b P. N. Lebedev Physical Institute, Moscow, Russia

Online Publication Date: 01 August 1993

To cite this Article: Igumenshchev, Igor V., Illarionov, Andrei F. and Kompaneets,

Dmitrii A. (1993) 'The outflow regime of quasispherical accretion onto a compact X-ray object', *Astronomical & Astrophysical Transactions*, 4:2, 91 - 105

To link to this article: DOI: 10.1080/10556799308205368

URL: <http://dx.doi.org/10.1080/10556799308205368>

PLEASE SCROLL DOWN FOR ARTICLE

Full terms and conditions of use: <http://www.informaworld.com/terms-and-conditions-of-access.pdf>

This article maybe used for research, teaching and private study purposes. Any substantial or systematic reproduction, re-distribution, re-selling, loan or sub-licensing, systematic supply or distribution in any form to anyone is expressly forbidden.

The publisher does not give any warranty express or implied or make any representation that the contents will be complete or accurate or up to date. The accuracy of any instructions, formulae and drug doses should be independently verified with primary sources. The publisher shall not be liable for any loss, actions, claims, proceedings, demand or costs or damages whatsoever or howsoever caused arising directly or indirectly in connection with or arising out of the use of this material.

THE OUTFLOW REGIME OF QUASISPHERICAL ACCRETION ONTO A COMPACT X-RAY OBJECT†

IGOR V. IGUMENSHCHEV,¹ ANDREI F. ILLARIONOV² and DMITRII A. KOMPANEETS²

¹*Institute of Astronomy, 48 Pyatnitskaya st., Moscow, 109017, Russia*

²*P. N. Lebedev Physical Institute, 84/32 Profsoyuznaya st., Moscow, 117810, Russia*

(6 August 1992)

We study numerically the quasispherical accretion of matter onto a relativistic object with anisotropic X-ray luminosity which is powered by this mass accretion. The X-rays heat the accreting gas through Compton scattering. When the gas temperature increases above the local escape temperature, a part of the accreting gas will flow outwards as a result of the action of the buoyancy force. The direction of the outflow coincides with the maximum of the X-ray luminosity. The depth of outflow as well as the velocity of the stream are correlated with the energy of X-ray quanta. The outflow is persistent, but the mass-loss rate is highly variable (~50%). In spite of the quantum nature of Compton heating, it markedly affects the gas, forcing the matter outflow even at X-ray luminosity as small as three order of magnitude less than the Eddington limit. The phenomena of hot gas outflow take place in the case of accretion onto a wind-fed X-ray source (neutron star or black hole) in a wide binary.

KEY WORDS accretion, X-ray star, hydrodynamics.

1. INTRODUCTION

Galactic X-ray binaries with the luminosity $L \sim 10^{36}$ erg s⁻¹ and active nuclei of galaxies and quasars with the hard X-ray and γ -ray luminosity $L \sim 10^{45}$ erg s⁻¹ seem to be fundamentally related to each other by the same process of energy release as a result of matter accretion onto the relativistic object (Zel'dovich and Novikov, 1971) of stellar mass $M = 1 \div 10M_{\odot}$ for a galactic source and $M \sim 10^9M_{\odot}$ for a QSO and AGN (Lynden-Bell, 1969). In spite of the enormous differences in mass and distance scales, the morphology of matter flows and accreting gas parameters in these objects are rather similar, which is a result of the following points:

- i. The luminosity of these objects in hard X-ray and soft γ bands is high ($L \gg 10^{-3}L_{\text{Edd}}$), roughly proportional to their mass M , and also variable and anisotropic. Here $L_{\text{Edd}} \approx 1.3 \cdot 10^{38}(M/M_{\odot})$ erg s⁻¹ is the limit Eddington luminosity. The gravitational energy of the infalling matter is converted into radiation in the immediate vicinity of the relativistic star, $r \sim 10^6(M/M_{\odot})$ cm: in

† This report is based mainly on the paper by Igumenshchev *et al.* (1992).

small regions (polar cups) on the surface of the magnetized neutron star or at distances about the inner radius of the accretion disc around a black hole. The small distance scales, mostly flat geometry, as well as the radiation transfer processes in the emission region explain both the hardness of the X-ray spectrum and the radiation anisotropy.

ii. The efficiency of the gravitational energy release for matter accretion at the rate \dot{M} onto the relativistic object is usually very high, $e = L/\dot{M}c^2 \sim 0.1$. For the neutron star of the mass $M_* = 1M_\odot$ and radius $r_* \approx 10^6$ cm (Baym and Pethick 1979) the efficiency $e = M_*G/(r_*c^2) \approx 0.15$ is of the order of the efficiency for disc accretion onto rotating black hole $e \approx 0.06 \div 0.42$ (Bardeen 1970). In both cases, it is much higher than $e \approx 10^{-4}$ for accretion onto a white dwarf of radius $r_* \approx 10^9$ cm and also much greater than $e \approx 0.007$ for the nuclear fusion reaction $H \rightarrow He$.

iii. An enormous number of hard quanta ($N_\nu/N_p \approx em_p c^2/\bar{\epsilon} \sim 10^4$ per accreting proton) of typical energy $\bar{\epsilon} \sim 10$ keV are radiated and pass through the accreting gas. These quanta intensively heat the gas through Compton scattering up to the particle energy equal to the "average" photon energy $\bar{\epsilon} \approx kT_C$ (Eq. (9)). The accreting matter, being hot and rarefied, will flow inwards quasispherically. However, in the case of rather higher luminosity $L > 10^{-3}L_{\text{Edd}}$ the accreting gas is overheated by radiation which results in a buoyancy-forced outflow; a part of the matter flows outwards in a direction correlated with the X-ray anisotropy (Illarionov and Kompaneets, 1990-Paper 1).

iv. The accretion morphology on any scale R mainly depends on the specific angular momentum of matter j at that distance. The maximum scale of the problem is the accretion radius (Eddington, 1926),

$$R_A = \frac{2MG}{w^2} \approx 3 \cdot 10^{10} \frac{M}{M_\odot} \text{ cm.} \quad (1)$$

In these calculations we use a typical wind velocity or velocity dispersion value $w \approx 10^8$ cm s $^{-1}$. Disc-like structures will be formed at R_A in the case $j \approx \sqrt{GMR_A}$. At $j \ll \sqrt{GMR_A}$ the flow pattern has a quasispherical character.

In this paper we study numerically the quasispherical matter accretion. Physically, this is the case of wide massive X-ray binaries (MXRB) where a compact star captures matter from a stellar wind from an OB companion (Davidson and Ostriker, 1973). More than half the observed X-ray pulsars are detected in such systems (Bradt and McClintock, 1983). This situation is also likely to occur at the scales of $R \sim 1$ pc for matter infall in slowly rotating nuclei of QSO and Seyfert galaxies. The quasispherical morphology of accretion flow is maintained from R_A down to the scale of the magnetospheric radius $r_H \approx 10^9$ cm of the neutron star or down to the scale $r_d \sim j^2/MG \ll R_A$ where the accretion disc around the relativistic star is eventually formed (due to non-zero angular momentum of the gas). In the case of a black hole, the formation of an accretion disc (if $j >> GM/c$) is of particular importance because only in this case do we expect the high luminosity efficiency $e \sim 0.1$. If no disc forms, then we do not expect a high X-ray luminosity from the black hole (Shapiro and Teukolsky, 1983). Matsuda *et al.* (1990) found the high amplitude $|j| \gg GM/c$ of variability of the angular momentum of matter captured from the stellar wind. In that case the

accretion disc of variable orientation can be formed allowing for a permanently high efficiency $e \sim 0.1$.

Bondi (1952) investigated the case of pure spherical accretion of matter when the effective index γ_e is less than the adiabatic one, $5/3$. This corresponds to the case of gas cooling. In the case of matter infall onto an X-ray source, the Compton heating increases the index γ_e above the adiabatic limit $5/3$ of the Bondi theory. This drastically changes the morphology of the accretion from a spherical infall to a quasispherical outflowing regime. When the X-ray luminosity is greater than the critical value (see below), the luminosity anisotropy forced the gas temperature in certain directions to be greater than the value of escape temperature T_{esc} (Eq. (6)). The overheated material is then pushed outwards by buoyancy force forming an outflow. An appropriate estimate of the depth of the outflow is the Compton radius (see Paper 1)

$$r_C = \frac{MGm_p}{5kT_C} \approx 3 \cdot 10^9 \left(\frac{M}{M_\odot} \right) \text{ cm}, \quad (2)$$

where the escape temperature T_{esc} of the gas is equal to the Compton temperature T_C (Eq. (9)) of X-rays. The radius r_C is much less than the accretion scale R_A in the case of hard X-rays with $kT_C > m_p w^2 / 10 \approx 1 \text{ keV}$ (for $w = 10^8 \text{ cm s}^{-1}$).

Ostriker *et al.* (1976), hereafter OMWY, discovered the paradox of the absence of solutions for steady spherical accretion of matter heated by X-rays of the luminosity $L > L_{\text{cr}} \approx 10^{-3} L_{\text{Edd}}$ through the Compton scattering. To solve this paradox, Bisnovatyi-Kogan and Blinnikov (1980), hereafter BB, drew attention to the free-free process of plasma cooling, which could fully compensate the Compton heating in the case of very slow matter settling and effectively made $\gamma_e = 5/3$. They found a steady spherical solution at $L > L_{\text{cr}}$. But Krolik and London (1983) indicate that this solution is thermally unstable for $l > L_{\text{cr}}$.

The paradox exists only in the case of pure spherical symmetry, and is a direct result of the one dimensional (radial) treatment of the accretion. However, in the general statement of the problem, the X-ray emission will not be isotropic. The anisotropy of emission causes the overheating of accreting matter in certain favoured directions. The accreting flow loses the spherical symmetry and transforms into quasispherical matter infall (see Paper 1) with a buoyancy forced matter outflow at the luminosity $L > L_{\text{cr}} \sim 10^{-3} L_{\text{Edd}}$; the same was found by OMWY. We did not succeed in constructing an analytical model of such accretion and were forced to go to numerical hydrodynamics. Two-dimensional computer models presented below conclusively show the existence of the outflow regime and enable us to analyse the parameters and features of the gas flow formed in these objects.

2. PHYSICAL PROCESSES IN THE MATTER ACCRETING ONTO AN X-RAY SOURCE

2.1. A Spherical Model of Adiabatic Gas Accretion

When the outflow is comparatively weak, $M_{\text{out}} < M_{\text{in}}$, which is typical in our conditions, the physical parameters of the accreting plasma are rather similar to

those in the model of steady spherical accretion. We use the spherical model for estimations of the plasma parameters in our nonspherical case.

In the case of the adiabatic spherical accretion of ionized hydrogen with $\gamma = 5/3$ the relationship between the plasma temperature T (or, precisely, the average temperature of electrons and protons $T = (T_e + T_p)/2$) and the velocity V is given by the Bernoulli equations: $V^2/2 + 5kT/m_p = GM/R$. The integration constant is omitted, which is valid for small R . The stationary solution of hydrodynamic equations (Bondi, 1952), satisfied by the Bernoulli equation, can be written in a parametric ($\alpha = \text{const}$) form

$$V = \alpha \sqrt{\frac{GM}{R}}, \quad T = \left(1 - \frac{\alpha^2}{2}\right) \frac{GMm_p}{5kR}, \quad 0 < \alpha < \sqrt{2}. \quad (3)$$

The density ρ or the number density $n = \rho/m_p$ of infalling matter is related to the accretion rate \dot{M} and to the total luminosity of the object $L = e\dot{M}c^2$ by the continuity equation

$$n = \frac{\dot{M}}{4\pi R^2 V m_p} = \frac{L}{4\pi R^2 V m_p c^2 e} \propto \frac{1}{\alpha e R^{3/2}}. \quad (4)$$

For $\alpha \sim 1$ the sound velocity in hydrogen plasma $v_s = (\gamma 2kT/m_p)^{1/2}$ is comparable with radial velocity V . The Mach number

$$\mathcal{M} = V/v_s = \alpha(3/(2 - \alpha^2))^{1/2} \sim 1 \quad (5)$$

and is radius independent. For $\alpha = \alpha_H = 1/\sqrt{2}$ (Hunt, 1971), the gas velocity V is equal to half the free-fall velocity $(2GM/R)^{1/2}$, the Mach number is $\mathcal{M} = 1$ and the temperature T is only 25% less than the escape temperature

$$T_{\text{esc}} = \frac{GMm_p}{5kR}. \quad (6)$$

Note that the ratio T/T_{esc} is constant in the spherical adiabatic model.

2.2. The Compton Heating and Buoyancy Forced Outflow

Consider the Compton heating of the accreting gas by X-rays from the accretion-powered central object. In the course of scattering, a fraction $\varepsilon^2/m_e c^2$ of the photon energy ε is gained by the electron due to the quantum effect of recoil. The rate of the Compton heating of electrons per unit plasma volume is proportional to the photon flux and to the energy gain and is given by

$$C^+ = \frac{n\sigma_T}{m_e c^2} \frac{\int \mathcal{L}(\varepsilon)\varepsilon d\varepsilon}{R^2}, \quad (7)$$

where $\sigma_T = 8\pi r_e^2/3 = 6.65 \cdot 10^{-25} \text{ cm}^2$, and $r_e = e^2/m_e c^2 = 2.83 \cdot 10^{-13} \text{ cm}$ are the Thomson scattering cross section and the radius of electron, $\mathcal{L}(\varepsilon)$ is the spectral luminosity of X-rays per unit solid angle Ω . The values of $\mathcal{L} = \int \mathcal{L}(\varepsilon) d\varepsilon$ and $L = \int \mathcal{L} d\Omega = e\dot{M}c^2$ are, respectively, the angular and the total luminosities of the central source. Combining the C^+ -term with the electron cooling rate $C^- =$

$4n\sigma_T kT_e \mathcal{L} / (m_e c^2 R^2)$, one has for the Compton mechanism (Peyraud, 1968)

$$C = C^+ - C^- = 3nk \frac{T_C - T_e}{t_C}. \quad (8)$$

Here the Compton temperature

$$T_C = \frac{\int \mathcal{L}(\varepsilon) \varepsilon d\varepsilon}{4k\mathcal{L}} \quad (9)$$

is determined by the ‘‘average’’ photon energy, the the Compton relaxation time is

$$t_C = \frac{3 m_e c^2 R^2}{4 \sigma_T \mathcal{L}}. \quad (10)$$

The temperature of the plasma T tends to approach the Compton temperature T_C : the radiation heats plasma with $T_e < T_C$ and cools it if $T_e > T_C$.

It should be noted that the Compton heating, in spite of its quantum nature, affects the flow much stronger than the classical force of radiation pressure,

$$\mathcal{F}_{\text{rad}} = \frac{\sigma_T \mathcal{L}}{cR^2}. \quad (11)$$

The ratio of the corresponding rates of energy gain $nV\mathcal{F}_{\text{rad}}/C^+ = m_e cV/4kT_e C \sim 2 \cdot 10^{-2}$ at the characteristic radius R_A (see Eq. (1)).

It was shown in Paper 1 that the condition of the outflow formation is when in some limited region the buoyancy force is greater than the gravity one, which is so when the plasma temperature exceeds the escape temperature,

$$T > T_{\text{esc}}. \quad (12)$$

This criterion is confirmed by numerical calculations (Section 5). To make the criterion specially adapted to the Compton heating, we can consider the plasma temperature growth in the course of steady radial matter infall due to compression and the Compton mechanism. The latter is responsible only for the growth in the ratio T/T_{esc} . This ratio increases most intensively at large radii $R \sim R_A$. The critical value of luminosity (numerically the same as in OMWY) which provides the growth of T/T_{esc} from the initial value $1 - \alpha^2/2$ at $R = R_A$ to $T/T_{\text{esc}} = 1$ inwards is (Paper 1)

$$\mathcal{L}_{\text{cr}} = \frac{3\sqrt{2} \alpha^3 w m_e c^2}{160 c k T_C} \mathcal{L}_{\text{Edd}} \sim 1.6 \cdot 10^{-3} \mathcal{L}_{\text{Edd}}, \quad (13)$$

where $\mathcal{L}_{\text{Edd}} = L_{\text{Edd}}/4\pi = GMcm_p/\sigma_T = 10^{37}(M/M_\odot)$ erg s⁻¹ ster⁻¹ is the Eddington luminosity per unit solid angle. Numerical factors are given here and below for $\alpha_H = 1/\sqrt{2}$, $w = 10^8$ cm s⁻¹, $kT_C = 10$ keV. Note that criterion $\mathcal{L} > \mathcal{L}_{\text{cr}}$ is more illustrative but is less precise than condition (12). The reason is a strong cubic dependence on α , whose value is specified rather arbitrarily at the outer boundary of the accretion flow.

The depth of the outflow r_C (see Eq. (2)) is estimated as the point where the matter escape temperature T_{esc} is equal to the Compton temperature T_C . Below

r_C , where $T_{\text{esc}} > T_C$, the Compton heating is unable to increase the plasma temperature to reach the escape value.

As shown by Igumenshchev *et al.* (1992), in the case of accretion-driven relativistic star with a very high efficiency of the gravitational energy release, $e \sim 0.1$, the Compton heating is the main mechanism of energy exchange between accreting plasma and radiation and the role of other mechanisms of plasma heating and cooling are negligible or (for electron thermal conductivity) at least limited. The lightest, electron component of plasma is responsible for the energy exchange between matter and radiation as heavy protons play the role of massive hot background. Our numerical models are constructed allowing for the two-temperature plasma approximation, which is suitable in the case when the thermal equilibrium of both components has time to be established, but the thermal energy exchange between electrons and protons could be suppressed. We consider a range of accretion rate parameters when this approximation is valid as well as the hydrodynamical treatment of the accretion is adequate.

3. NUMERICAL METHOD

The algorithm of calculation described in Harten *et al.* (1987) and Harten and Osher (1987) forms the basis for our numerical method. Namely, we use an explicit second-order Eulerian method, which is a modification of the well-known Godunov (1959) scheme. Briefly, we are modeling the time evolution of the system which is described by hydrodynamic equations in the conservative form. The finite-difference representation for these equations is made for the functions which are approximated by piecewise-linear distributions. In the determination of the system's state at a moment $t+h$ (where h is the time step), in terms of the known state at the moment t , the fluxes of hydrodynamic functions (density, momentum and energy) at the boundaries of numerical cells at the moment $t+h/2$ have been used. These fluxes are obtained by solving the Riemann problem (Godunov *et al.*, 1968).

We suppose for simplicity that the matter accreting onto the central object is a fully ionized hydrogen plasma with the adiabatic index $\gamma = 5/3$. The description of its dynamics is made in the frame of two-temperature (T_p , for protons and T_e , for electrons), quasineutral ($n_p = n_e = n$) plasma approximation. In the case of azimuthal symmetry and in the absence of angular momentum in the accreting matter the flow is described in cylindrical coordinates (r, z) by the following system of equations:

a) mass conservation,

$$\frac{\partial \rho}{\partial t} + \frac{1}{r} \frac{\partial}{\partial r} (r \rho u) + \frac{\partial}{\partial z} (\rho v) = 0, \quad (14)$$

b) momentum,

$$\frac{\partial}{\partial t} (\rho u) + \frac{1}{r} \frac{\partial}{\partial r} (r \rho u^2) + \frac{\partial}{\partial z} (\rho uv) = - \frac{\partial P}{\partial r} - \left(1 - \frac{\mathcal{L}(\theta)}{\mathcal{L}_{\text{Edd}}} \right) \frac{GM\rho}{R^2} \sin \theta, \quad (15)$$

$$\frac{\partial}{\partial t} (\rho v) + \frac{1}{r} \frac{\partial}{\partial r} (r \rho vu) + \frac{\partial}{\partial z} (\rho v^2) = - \frac{\partial p}{\partial z} - \left(1 - \frac{\mathcal{L}(\theta)}{\mathcal{L}_{\text{Edd}}} \right) \frac{GM\rho}{R^2} \cos \theta, \quad (16)$$

c) total energy $E = \rho(u^2 + v^2)/2 - \rho GM/R + \varepsilon_e + \varepsilon_p$ of the plasma,

$$\begin{aligned} \frac{\partial E}{\partial t} + \frac{1}{r} \frac{\partial}{\partial r} (ru(E + P)) + \frac{\partial}{\partial z} (v(E + P)) \\ = C - B + \frac{\mathcal{L}(\theta)}{\mathcal{L}_{\text{Edd}}} \frac{GM\rho}{R^2} (u \sin \theta + v \cos \theta), \end{aligned} \quad (17)$$

d) internal energy ε_e of the electron component,

$$\frac{\partial \varepsilon_e}{\partial t} + \frac{1}{r} \frac{\partial}{\partial r} (ru\varepsilon_e) + \frac{\partial}{\partial z} (v\varepsilon_e) = -P_e \left(\frac{1}{r} \frac{\partial}{\partial r} (ru) + \frac{\partial v}{\partial z} \right) + C - B - Q, \quad (18)$$

e) equation of state

$$P_e = \frac{2}{3}\varepsilon_e, \quad P_e = nkT_e, \quad P_p = \frac{2}{3}\varepsilon_p, \quad P_p = nkT_p. \quad (19)$$

Subscripts “e” and “p” are used here for electron and proton gases, respectively, $\rho = nm_p$ is the mass density and n is the number density of plasma particles, u and v are the r and z components of the velocity, $P = P_e + P_p$ is the plasma pressure, $R = \sqrt{r^2 + z^2}$ is the modulus of the radius vector, θ is the angle between the radius vector and the z -axis, $0 \leq \theta \leq \pi$, $\mathcal{L}(\theta)$ is the angular distribution of the X-ray luminosity of the central source. The term with $\mathcal{L}(\theta)/\mathcal{L}_{\text{Edd}}$ in Eqs (15)–(17) accounts for the correction for the radiative pressure force (Eq. (11)). The total luminosity $L = 2\pi \int_0^\pi \mathcal{L}(\theta) \sin \theta d\theta$ is determined by the momentary mass accretion rate \dot{M}_{in} through the inner boundary (see the next section) and by the efficiency of the accretion e , with

$$L = e\dot{M}_{\text{in}}c^2. \quad (20)$$

For numerical calculations we choose $e = 0.15$. The main processes of heat exchange are taken into account in Eqs. (17) and (18). The Compton term C is given by Eq. (8). For the Bremsstrahlung term B , see Heitler (1944), and for the energy transfer from electrons to protons, Q see Landau and Lifshitz (1981). We suppose for simplicity that the Compton temperature T_C in the C term is angle independent. We choose $kT_C = 10$ keV. Note that Coulomb collisions (Q) do not change the total energy of the plasma (Eq. (17)), so the appropriate term is present only in Eq. (18) for the internal energy of the electron component.

For the angular distribution of the luminosity of the central source, we adopt one of the two forms. The first one is a narrow bipolar Gaussian,

$$\mathcal{L}(\theta) = \begin{cases} L \exp\{-(\theta/\Delta\theta)^2\}/4\pi I, & \text{for } 0 \leq \theta < \pi/2, \\ \mathcal{L}(\pi - \theta), & \text{for } \pi/2 \leq \theta < \pi, \end{cases} \quad (21)$$

where $\Delta\theta$ is the width of the beam, with the normalisation constant

$$I = \int_0^{\pi/2} \exp\{-(\theta/\Delta\theta)^2\} \sin \theta d\theta \approx 0.5 \Delta\theta \sin \Delta\theta \quad \text{for } \Delta\theta < 1.$$

The second distribution has wide wings and an isotropic component:

$$\mathcal{L}(\theta) = \frac{L}{4\pi} ((1 - \chi) \cdot 3 \cos^2 \theta + \chi), \quad 0 \leq \chi \leq 1. \quad (22)$$

Thermal exchange processes are introduced in the numerical scheme by means of the operator splitting method (Marchuk, 1977). At the beginning of each cycle of calculation (i.e., the calculation of the hydrodynamic evolution on a time step h), the temperatures of electrons and protons are determined, which have been established as a result of processes C , Q and B at a time step h . This calculation is made with a given matter distribution, without taking into account the plasma motion. Next the calculation of the hydrodynamics cycle is performed. In this case thermal processes C , Q and B are not taken into account. As a result, the new state of the system at time $t + h$ is obtained.

Calculations were made on a spatially homogeneous grid. The additional assumption of the mirror symmetry (relative to the $z = 0$ plane) allowed us to make calculations in one quadrant of the meridional cross section of the size 200×200 mesh points. The time step h was calculated according to the well-known Courant condition for explicit schemes (Courant, Friedrichs and Lewy, 1928).

4. BOUNDARY CONDITIONS

The problem of boundary conditions may be divided into two parts. The first one is the prescription of the conditions at the outer boundary of the grid. These conditions must allow for both an outflow and inflow of the matter. The second part is the setting of an absorption conditions for the accreting matter at the inner boundary which have to model the hydrodynamics in the vicinity of the central gravitating object.

4.1. The Outer Boundary

Firstly we set the criterion which permits the determination of the regions of matter outflow and inflow through the outer boundary: if the temperature of the plasma $T_B = \frac{1}{2}(T_e + T_p)|_B$ at the outer boundary (at the distance R_B from the centre) exceeds the corresponding escape temperature T_{esc} (Eq. (6)), then the condition of the outflow of the heated gas is satisfied (see Paper 1), otherwise (at $T_B < (T_{\text{esc}})_B$) the inflow takes place. Obviously, this criterion is only approximate in the case of unsteady and non-spherical accretion. But it is in a qualitative agreement with the results for a spherical model (see Eq. (3)). Steady accretion does not occur if $T > T_{\text{esc}}$.

For convenience, we use artificial cells which border with the region of calculation. The set of the boundary condition in this case reduces to the set of values of the velocity, density and temperature of the plasma in the artificial cells in the beginning of each time-step calculation. A free outflow (for $T_B > (T_{\text{esc}})_B$) is simulated by giving the value of the velocity, density and temperature of the gas in the artificial cells to be the same as at the boundary.

The definition of the conditions of matter inflow through the outer boundary (for $T_B < (T_{\text{esc}})_B$) is the following. By using the value of the gas temperature in the boundary cells, we calculate the quantity

$$\tilde{\alpha} = \min\{\alpha_T, \alpha_0\}, \quad \alpha_T = (2 - 2T_B/(T_{\text{esc}})_B)^{1/2}. \quad (23)$$

In our calculation, we take $\alpha_0 = 0.4$ (from the range $0 \div \sqrt{2}$) which corresponds to the maximum possible value of the Mach number $\mathcal{M} = 0.51$ (i.e., we restrict the regime of accretion near the boundary to be subsonic). Next we substitute $\bar{\alpha}$ instead of α into Eqs (3) of the spherical model, and determine the velocity and the temperature of matter in the artificial cells (which border a given boundary cell). The density of inflowing plasma, which is specified in the artificial cells and is independent of time and boundary condition, is determined by

$$\rho_B = \frac{\dot{M}_0}{4\pi R_B^2 \alpha_0 \sqrt{\frac{GM}{R_B}}}, \quad (24)$$

where \dot{M}_0 is the chosen typical accretion rate. The rate of matter input at the outer boundary is limited to be less than \dot{M}_0 .

4.2. The Inner Boundary

At the inner boundary of the numerical grid, at $R = R_{in}$ with $R_{in} < r_C$, where the Compton cooling is rather effective, we use the condition of complete absorption, in which the plasma passes through the inner boundary but neglecting any influence of pressure from the lower layers. It is better to say that it is a sucking boundary. This condition is similar to the one used by Hunt (1971) in the numerical computation of the Bondi accretion.

The set of absorbing boundary conditions at some radius R_{in} is an adequate representation of reality only in the case of supersonic accretion in the inner region, when the transfer of any perturbation outwards is impossible and the influence of a real boundary on the inflow can be neglected. The supersonic accretion can take place in a cooling flow, when the cooling processes in the shocked gas close to the real inner boundary at R_{real} (at the radius of the magnetosphere of a neutron star, for instance) is so efficient that the shock wave cannot propagate outwards from this boundary. This is the case when the Compton cooling time t_C (Eq. (10)) at $R \approx R_{real}$ is less than the time of gas motion below the shock through the hot shocked layer, $t_d = \Delta R / V_{sh}$, where ΔR is the width of the heated layer and V_{sh} is the gas velocity below the shock. Evaluating this dynamic time as the infall time $R^{3/2} / \sqrt{MG}$ at $R = R_{real}$, we compare it with the Compton time and obtain a criterion for the rate of accretion (or, precisely, the luminosity), at which the inflow can be described using the absorbing inner boundary condition:

$$L > L_{abs} = \frac{3\pi m_e c^2}{\sigma_T} \sqrt{GMR_{real}}. \quad (25)$$

If this inequality is satisfied, we can formulate the absorbing boundary condition at R_{in} somewhere in the region $r_C > R_{in} > R_{real}$, hoping it is adequate. For instance, in the problem of accretion onto a neutron star magnetosphere of the radius $r_H \sim 10^9$ cm the absorbing boundary condition at $R_{real} \approx r_H$ is adequate for $L > 3 \cdot 10^{36}$ erg s⁻¹.

Otherwise (at $L < L_{abs}$), the absorption boundary conditions at any R_{in} are not

a representation of the real conditions.† In this case more complex boundary conditions have to be used. Any possible kind of boundary conditions will affect the flow parameters in its own specific manner. In this low-luminosity case, shocks (a time sequence of shocks) quasiperiodically move outwards away from the boundary R_{real} , heat the accreting matter and establish a subsonic regime of accretion, at least for a while.

Note that $R_{\text{real}} > 2MG/c^2$ and therefore L_{abs} is at least m_e/m_p times L_{Edd} , and the criterion for outflow ($L > 10^{-3}L_{\text{Edd}}$) is definitely satisfied when the absorbing inner boundary condition holds. And finally, the instantaneous accretion rate onto the central object \dot{M}_{in} in our computations is determined at the inner boundary. This value is used to calculate the total luminosity L using Eq. (20).

5. RESULTS

Igumenshchev *et al.* (1992) discuss the results of calculations for three hydrodynamic models, performed on the same grid, with the “absorbition” type inner boundary conditions for the mass of the central object $M = 1M_{\odot}$, the accretion efficiency $e = 0.15$, and the Compton temperature $kT_{\text{C}} = 10$ keV. The outer boundary of the calculation region is taken on a square (which is caused by the adoption of cylindrical coordinates in the numerical method). The closest point of the outer boundary is placed at the distance $R_{\text{A}} = 3 \cdot 10$ cm $\approx 10r_{\text{C}}$ from the center, the Compton radius is $r_{\text{C}} \approx 2.8 \cdot 10^9$ cm, the inner boundary is placed at $R_{\text{in}} \approx 8 \cdot 10^8$ cm $\approx 0.3r_{\text{C}}$.

In *Model 1* and *Model 2* we chose the same parameter $\dot{M}_0 = 10^{-10}M_{\odot}/\text{yr}$ (see Eq. (24)). In *Model 3*, this is 5 times larger, $\dot{M}_0 = 5 \cdot 10^{-10}M_{\odot}/\text{yr}$. The anisotropy of luminosity for each model is specified and fixed during the calculation. For *Models 1* and *Models 2*, the anisotropy is given by Eq. (22) with $\chi = 0$ for *Model 1*, and $\chi = 0.5$ for *Model 2*. *Model 3* has a Gaussian anisotropy (Eq. (21)) with $\Delta\theta = \pi/8$.

The recalculation of the results for the central mass differing from $M = 1M_{\odot}$ for each model is trivial and reduces to the scaling of all the parameters (the characteristic distance, time scale, \dot{M}_0 (see above), and also the resulting accretion rate \dot{M}_{in} , outflow rate \dot{M}_{out} and luminosity L) by the same factor M/M_{\odot} .

Unstable structures such as outgoing shocks and vortex rings appear quasiperiodically in the large-scale accretion flow and outflow. Unsteady processes do not affect significantly the accretion rate \dot{M}_{in} (the variations of the accretion rate is only about a few percent). In contrast, these processes have a strong effect on the outflow rate \dot{M}_{out} , which oscillates during the time evolution with the amplitude of tens percent. Oblique shocks (see Landau and Lifshitz, 1959) appear near the base of the outflow at the distances somewhat larger than r_{C} . The action of these oblique shocks results in the collimation of the accretion flow towards the center. During the outward propagation of the oblique shocks, a transverse shock appears on the closest to the central object region.

† Any numerical results for matter accretion onto a relativistic star which have been performed with the absorbition (sucking) inner boundary condition, which pretended to be hydrodynamically pure, but did not take into account the back influence of the luminosity on the matter flow, are incomplete.

Some vortex rings appear during the evolution at the border between the outflow and inflow regions. Their seeds originate at the distance $R_{\text{rot}} \approx 3r_c \approx 10^{10}$ cm, which is far from the outer boundary ($R_A = 3 \cdot 10^{10}$ cm).

To illustrate the outflow pattern, we present some results for the *Model 1* at an arbitrarily chosen calculation time.

The figures present the structure of the *Model 1* at time $t = 2224$ s which is seven times the characteristic free-fall time $t_{\text{ff}} = R_A/w$. Four maps of density and velocity distributions, Mach number, pressure and relative temperature are presented in the plane of meridional section of the gas flow. The axis Y coincides with the symmetry axis and the emission of the central object is concentrated near this direction. The axis X is placed in the equator plane. The compact object is in the center. The scales of the axes X and Y are given in units of 10^9 cm (for an object with the mass $M = 1M_\odot$).

Figure 1: Curves of constant density and velocity field (arrows). The constant-density lines are spaced by $\Delta \lg \rho = 0.1$. The direction and the length of the arrows correspond to the matter velocity vectors at their positions. The minimal level of the outflow is reached on the axis at $Y = \pm 3.43 \cdot 10^9$ cm. The outflow rate is $\dot{M}_{\text{out}} = 5.96 \cdot 10^{14}$ g/s at the outer boundary. The accretion rate onto the central object is $\dot{M}_{\text{in}} = 4.15 \cdot 10^{15}$ g/s. The transverse shock front can be clearly seen in this figure (at $X \approx \pm 1 \cdot 10^{10}$ cm, in the equatorial plane), in addition to oblique shocks crossing at $X \approx \pm 1.5 \cdot 10^{10}$ cm, $Y = 0$). The equatorial accretion flow

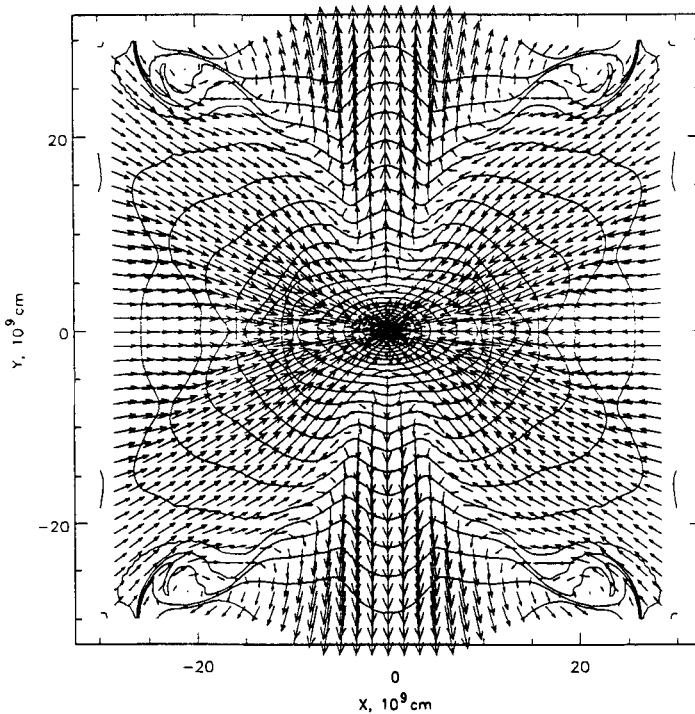


Figure 1 The map of constant density and velocity in model 1.

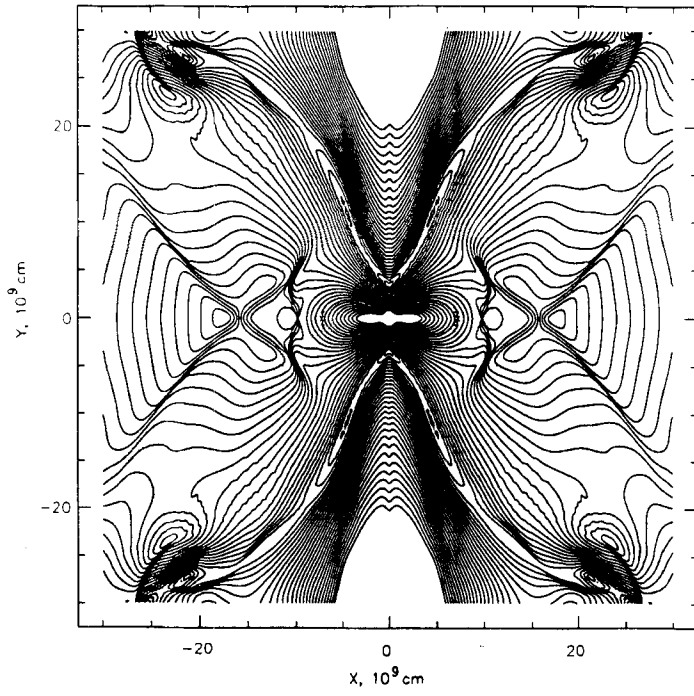


Figure 2 The map of constant Mach number.

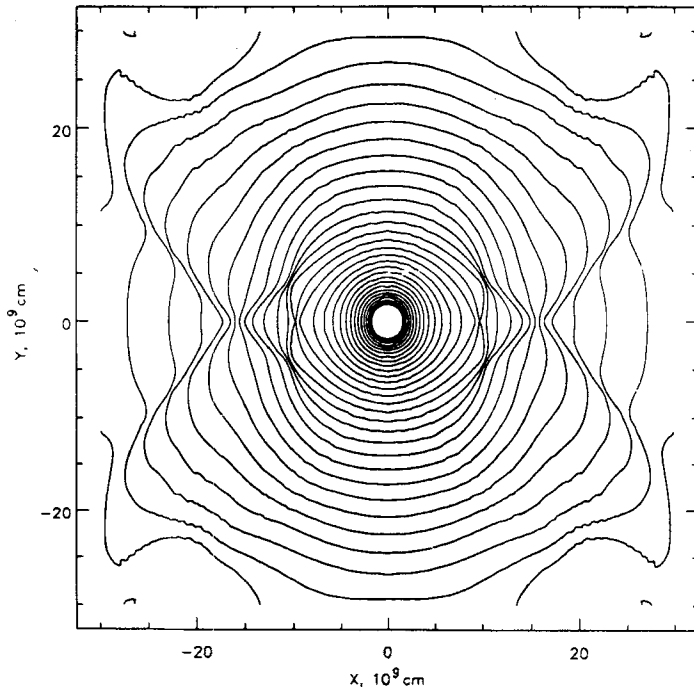


Figure 3 The curves of constant pressure.

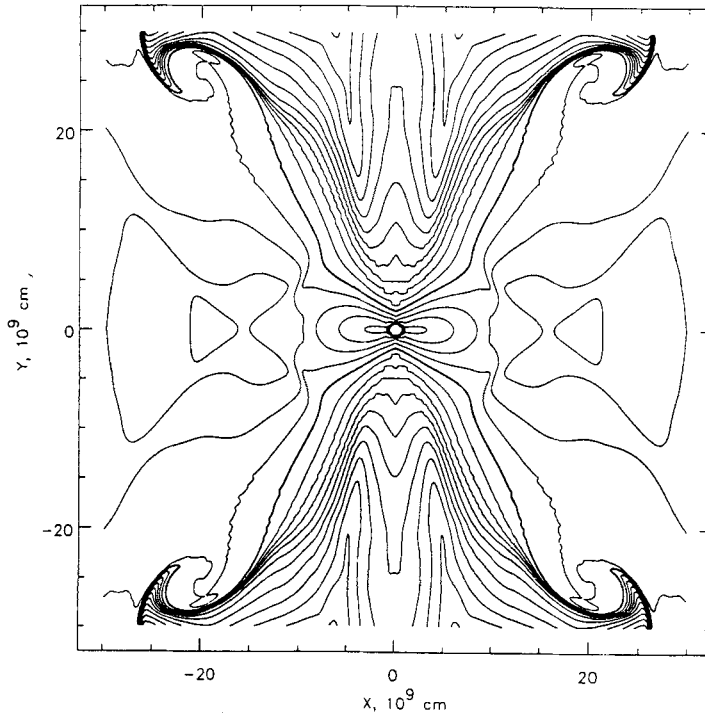


Figure 4 The map of constant temperature ratio T/T_{esc} , the contour $T/T_{\text{esc}} = 1$ is shown by the thick lines.

becomes subsonic after the pass of the oblique shock and accelerates again up to supersonic velocities passing through the points $X \approx \pm 7 \cdot 10^9$ cm (in the equatorial plane) before reaching the Compton cooling region ($R < r_C$). Vortex rings can be seen at $X, Y \approx 2 \cdot 10^{10}$.

Figure 2: The map of constant Mach number \mathcal{M} , with the step $\Delta \mathcal{M} = 0.05$. The pattern consists of the central summit (hill), stretched along the equator (the value $\mathcal{M} = 1$ is marked by a circle at $X \approx 1.25 \cdot 10^9$ cm). Equatorial and axial hills are separated by hollows, which originate at stagnation points ($Y \approx \pm 3 \cdot 10^9$ cm) with $\mathcal{M} = 0$.

Figure 3: Curves of constant pressure P . The step is $\Delta \lg P = 0.1$. The summit here is the central peak.

Figure 4: The map of constant temperature ratio T/T_{esc} . Contours are spaced by $\Delta(T/T_{\text{esc}}) = 0.1$, the value $T/T_{\text{esc}} = 1$ is marked by thick curves. The pattern consists of the equatorial cavity ($T/T_{\text{esc}} < 1$) and smooth rises with Y increasing.

6. DISCUSSION

We have studied the quasispherical accretion of matter onto a compact X-ray source. The calculation of two-dimensional axisymmetric models of accreting

objects accounts for the interaction of plasma with X-rays. We have shown that regions with outflow exist in addition to accretion regimes. The outflow is a result of the Compton heating of the accreting plasma through the scattering of X-rays and the buoyancy force action on the overheated gas. The anisotropy of the radiation determines the direction of the outflow. The outflowing matter accounts for about $\approx 10\%$ of the accreting matter. This value is large enough to prevent the Compton overheating of the main infalling part of matter. The flow is nonstationary; vortices form quasiperiodically at the border between the outflow and the accretion region, shocks also form and move outwards. Note that these nonstationarities only weakly affect the variability of the accretion luminosity of the central object.

The hardness of the radiation is essential as it is correlated with the depth of the outflow r_C . The outflow velocity is correlated with the gas sound velocity at temperature T_C , and so the particle kinetic energy in the outflow is comparable with the average energy of quanta. The outflow is formed if the accretion efficiency is high, $e \gg 10^{-3}$. This is the case of matter infall onto a relativistic star only, e.g., X-ray objects in massive binaries and super-massive black holes in QSO and AGN.

However, in the case of a very slow stellar wind, $w < 100 \text{ km s}^{-1}$, as in the red giant case, the gas temperature behind the shock, at the R_A scale, is very small and recombination cooling will control the morphology and gas dynamics of accreting flows leading to a narrow cone-like accretion column. The Compton heating is unable to form a massive outflow in this case. The same will be in the case of matter accretion onto a white dwarf. The efficiency of emission, $e \approx 10^{-4}$, is small and bremsstrahlung (at $T > 10^6 \text{ K}$) or recombination (at $T < 10^6 \text{ K}$) are the main cooling processes controlling the plasma thermal balance.

The outflow regime of accretion onto a magnetized neutron star explains the phenomena of long-periodic (100 ÷ 1000 s) wind-fed X-ray pulsars in wide massive binaries with OB star (see Paper 1). The matter captured from wind of the OB star accretes quasispherically onto the neutron star. The outflow can start deep enough to touch the upper boundary of the magnetosphere of the neutron star and drags magnetic lines into the outflow. The neutron star and its magnetosphere corotate, so shearing of the captured magnetic field by the outflow provides the transfer of the angular momentum from the pulsar to the outflowing matter, causing the neutron star to spin down.

References

- Bardeen, J. M. (1970). *Nature*, **226**, 64.
 Baym, G. and Pethick, C. (1979). *Ann Rev. Astr. Astrophys.*, **17**, 415.
 Bisnovatyi-Kogan, G. S. and Blinnikov, S. I. (1980). *Mon. Not. R. astr. Soc.*, **191**, 711 (BB).
 Bondi, H. (1952). *Mon. Not. R. astr. Soc.*, **112**, 195.
 Bradt, H. V. D. and McClintock, J. E. (1983). *Ann. Rev. Astr. Astrophys.*, **21**, 13.
 Courant, R., Friedrichs, K. O. and Lewy, H. (1928). *Math. Ann.*, **100**, 32.
 Davidson, K. and Ostriker, J. P. (1973). *Astrophys. J.*, **179**, 585.
 Eddington, A. S. (1926). In: *The Internal Constitution of the Stars*, p. 391, Cambridge University Press, Cambridge.
 Godunov, S. K. (1959). *Matematich. Sbornik*, **47**, 271 (in Russian).
 Godunov, S. K., Zabrodin, A. V., Ivanov, M. Y., Krayko, A. N. and Prokopov, G. P. (1968). In: *Numerical Solving of Multidimensional Gasdynamics Problems*, chap. 2, ed Godunov, S. K., Nauka, Moscow (in Russian).

- Harten, A., Engquist, B., Osher, S. and Chakravathy, S. R. (1987). *J. Comput. Phys.*, **71**, 231.
- Harten, A. and Osher, S. (1987). *SIAM J. Numer. Anal.*, **24**, 19.
- Heitler, W. (1944). In: *The quantum theory of Radiation*, p. 172, Oxford University Press, Oxford.
- Hunt, R. (1971). *Mon. Not. R. Astr. Soc.*, **154**, 141.
- Illarionov, A. F. and Kompaneets, D. A. (1990). *Mon. Not. R. Astr. Soc.*, **247**, 219 (Paper 1).
- Igumenshchev, I. V., Illarionov, A. F. and Kompaneets, D. A. (1993). *Mon. Not. R. Astr. Soc.*, in press. (Institute of Astronomy, Cambridge, 1991, preprint).
- Krolik, J. H. and London, R. A. (1983). *Astrophys. J.*, **267**, 18.
- Landau, L. D. and Lifshitz, E. M. (1981). In: *Course of Theoretical Physics. v.10. Physical Kinetics*, p. 174, Pergamon Press, Oxford.
- Landau, L. D. and Lifshitz, E. M. (1959). In: *Course of Theoretical Physics. v.6. Fluid Mechanics*, p. 333, p. 349, Pergamon Press, Oxford.
- Lynden-Bell, D. (1969). *Nature*, **223**, 690.
- Marchuk, G. I. (1977). *Methods of Numerical Mathematics*. Nauka, Moscow.
- Matsuda, T., Sekino, N., Sawada, K., Shima, E., Livio, M., Anzer, U. & Börner, G. (1990). Preprint MPA 540.
- Ostriker, J. P. McCray, R., Weaver, R. and Yahil, A. (1976). *Astrophys. J. Lett.*, **208**, L61 (OMWY).
- Peyraud, J. (1968). *Journal de Physique*, **29**, 88.
- Shapiro, S. L. and Teukolsky, S. A., 1983. In: *Black Holes, White Dwarfs, and Neutron Stars*, p. 427, John Wiley and Sons, Inc., New York.
- Zel'dovich, Ya. B. and Novikov, I. D. (1971). In: *Relativistic Astrophysics. v. 1.*, chap. 13, University of Chicago Press, Chicago.